Research papers

Assessment of remotely-sensed sea-surface temperature and chlorophyll-*a* concentration in San Matías Gulf (Patagonia, Argentina)

Gabriela N. Williams [a,d,*], A.I. Dogliotti [b,d], P. Zaidman [c,d], M. Solis [a,d], M.A. Narvarte [c,d], R.C. González [c,d], J.L. Esteves [a,d], D.A. Gagliardini [a,b,d]

[a] Centro Nacional Patagónico (CENPAT), Boulevard Brown 2915, (U9120ACV)—Puerto Madryn, Chubut, Argentina
[b] Instituto de Astronomía y Física del Espacio (IAFE), Ciudad Universitaria, Ciudad Autónoma de Buenos Aires, Argentina
[c] Instituto de Biología Marina y Pesquera Almirante Storni (IBMPAS), Güemes 1030, (8520) San Antonio Oeste, Río Negro, Argentina
[d] Consejo Nacional de Investigaciones Científicas y Técnicas (CONICET), Argentina

ARTICLE INFO

ABSTRACT

Field measurements of surface temperature and chlorophyll-*a* concentration were used to evaluate for the first time the performance of the standard sea surface temperature and chlorophyll-*a* algorithms of the Moderate Resolution Imaging Spectroradiometer (MODIS) in San Matías Gulf, northern of the Argentine Patagonian Continental Shelf (between 40°47′S and 42°13′S). The fit of the temperature data to a Standard Major Axis (SMA) type II regression model indicated that a high proportion of the total variance ($r^2 \geq 0.80$) was explained by the model. For chlorophyll-*a*, the low correlation ($r^2 = 0.15$) and high dispersion indicated a poor performance and a general overestimation of Chl-*a* by the OC3Mv5 algorithm as indicated by the Relative Percent Difference (RPD=113%). However, for stations located in the northern area of the gulf the result showed a higher correlation ($r^2 = 0.76$) and less dispersion (RPD=31%). The feasible reasons and explanations for the performance of NLSST and OC3Mv5 algorithms are discussed. The results of the temporal variability analysis of SST and Chl-*a* in different areas of the gulf agreed with previous studies.

© 2012 Elsevier Ltd. All rights reserved.

1. Introduction

Remote sensed data of infrared and ocean color have shown to be a useful tool for monitoring the marine ecosystem. It has provided near real-time, long-term and synoptic global estimates of key parameters, such as sea surface temperature (SST) and chlorophyll-*a* (Chl-*a*), which can be integrated in numerical weather prediction, basin-scale hydrodynamics and primary production models (Longhurst et al., 1995; Behrenfeld and Falkowski, 1997).

The Advanced Very High Resolution Radiometer (AVHRR) sensor, onboard NOAA satellites, is the most used in the estimation of SST for scientific and operational applications in oceanography and fisheries. Bava (2004) found a significant correlation between *in-situ* temperature and estimates by the AVHRR sensor over the Southwest Atlantic (SWA). At present, a relatively new sensor, the Moderate Resolution Imaging Spectroradiometer (MODIS) onboard the satellite Aqua (launched in May 2002) has the advantage of estimating both SST and Chl-*a* simultaneously.

Although several studies have analyzed the spatial and temporal distribution of MODIS SST and Chl-*a* in the SWA (Saraceno and Piola, 2005; Barré et al., 2006), SST algorithms have not been evaluated in this region.

Records of satellite-derived Chl-*a* began in 1978 with the Coastal Zone Color Scanner sensor (CZCS) and finished in 1986 (Gordon and Clark, 1980; Hovis et al., 1980; Feldman et al., 1989). After a decade more sophisticated sensors were put into orbit, including SeaWiFS (Sea-viewing Wide Field of view Sensor) currently out of operation, MERIS (MEdium Resolution Imaging Spectrometer), whose mission has recently ended, and MODIS-Aqua and MODIS-Terra sensors which are currently operational. Global algorithms of chlorophyll-*a* have been empirically derived from a large *in-situ* database collected in waters around the world (O'Reilly et al., 1998, 2000; Morel and Antoine, 2002). These empirical algorithms rely on mean statistical relationships between chlorophyll-*a* concentration and the blue-to-green reflectance ratio, and hold true in case 1-waters according to the classification introduced by (Morel and Prieur, 1977) and refined later by Gordon and Morel (1983). The presence of phytoplankton with a different pigment composition from that used to build the empirical algorithms may cause such relationship to break down. Furthermore, deviations from standard relationships could be caused by the presence of optically active

components other than chlorophyll-*a* which do not co-vary with it. Global algorithms work well in some regions, especially where the *in-situ* data were obtained to build the algorithms (Bailey et al., 2000; Hooker and McClain, 2000). However, they have been shown to be less suitable in other parts of the world (Fuentes-Yaco et al., 2005). Bio-optical measurements and SeaWiFS Chl-*a* algorithm performance have been analyzed and regional algorithms have been suggested in the northern part of the Argentine shelf (Lutz et al., 2006, Garcia et al., 2005, 2006). More recently, Dogliotti et al. (2009) evaluated global and regional algorithms in the Patagonian Continental Shelf and found that the global algorithms performed better and within the accuracy of the algorithm itself, *i.e.* similar RMSE to that obtained when the algorithm was derived using *in situ* measurements.

The San Matías Gulf (SMG) is a semi-enclosed basin with singular features located in the north of the Patagonian Continental Shelf between 40°47′S and 42°13′S (Fig. 1a). It is the second largest gulf of the Argentine Continental Shelf, covering an area of approximately 20,000 km^2. Around 55% of the gulf is deeper than 100 m, with a maximum depth of 180 m in the central area. The continental shelf on the eastern side of the Gulf forms an open basin with a mean depth of 70 m (Fig. 1b). Even though there is no direct river discharge into the gulf, its northern part is influenced by the Negro river, which has a flow rate of about 1000 m^3 s^{-1}(Guerrero and Piola, 1997). This river is primarily used for agriculture, livestock and other urban activities. Precipitation in this zone is typical of a semi-arid region (250 mm year^{-1}), with predominantly western winds (Hoffmann et al., 1997).

Studies carried out in SMG through oceanographic surveys between 1971 and 1994 showed the presence of two distinct areas from November to March (Carreto et al., 1974a, 1974b; Scasso and Piola, 1988; Rivas and Beier, 1990; Williams, 2004; Williams et al., 2010). Piola and Scasso (1988) described a thermal front during the Austral Summer, located around 41°50′S (from west to east), which separates two areas. This front (red dashed line in Fig. 1a) has been also identified using AVHRR thermal data (Rivas and Dell'Arciprete, 2000; Bava et al., 2002). Moreover, brightness temperature maps from Landsat Thematic and Enhanced Thematic Mapper (TM/ ETM+) images corresponding to Spring–Summer months revealed a SST distribution characterized by the presence of another thermal front over the northern half of the mouth (blue dashed line in Fig. 1a) (Gagliardini and Rivas, 2004). The tidal energy flow at the mouth of SMG is one of the highest in the world (Tonini et al., 2007) and the Simpson–Hunter criterion indicates vertical mixing in this region (Palma et al., 2004).

Thus, in summer, the SMG is more isolated from the continental shelf, showing two different regions according to the properties of the water masses. Also, the northern area of the gulf is more isolated, stratified and with higher temperature and salinity than the southern area (Rivas and Beier, 1990). The latter is influenced by southern intrusions of water from the shelf, which result in high nitrate concentrations and less stratification (Williams, 2004). Satellite data showed an average difference of 1–3 °C in SST in summer between the northern and southern areas, while in winter, when the thermal front vanishes, the SST distribution is spatially homogeneous (Piola and Scasso, 1988; Gagliardini and Rivas, 2004).

The SMG is an important area for fisheries, being the Argentine hake (*Merluccius hubbsii*) the most important fishery in terms of landings and economical revenues (González et al., 2007; Romero et al., 2010; Ocampo-Reinaldo, 2010). The spatial and temporal patterns of temperature and chlorophyll-*a* are important characteristics of fisheries ecosystems, and have implications for a sustainable management of fisheries and aquaculture (Santos, 2000; Williams et al., 2010). Thus, remote sensing methods constitute an efficient way to improve the knowledge of the environmental conditions of this ecosystem and have been used with increasing success to confirm previous oceanographic findings (Gagliardini and Rivas, 2004; Williams et al., 2010). However, it is necessary to assess the accuracy of the estimations. In a previous study a comparison between SeaWiFS and *in situ* Chl-*a* values in the SMG showed a poor performance of the standard algorithm (OC4v4) and a good performance of NOAA-AVHRR SST estimates in this region (Williams et al., 2010). Thus, SMG is a very interesting basin to develop and assess sea surface and ocean color products in the framework of the ECOPES project (PID 371, 2003), with the aim of applying remote sensing data in the environmental characterization of regional and coastal seas. The SMG ecosystem is the main source of goods and services for several Patagonian coastal communities and it supports human activities based on the exploitation of fishery resources and tourism. Moreover, several coastal regions constitute Marine Protected Areas, being the most prominent the Peninsula Valdés, which achieved the status of Natural Patrimony of Humanity.

The aims of this work are to compare the values obtained from the existing standard MODIS algorithms of sea-surface temperature (SST) and chlorophyll-*a* concentration (Chl-*a*) with *in-situ* measurements in SMG; and to study the temporal variability of SST and Chl-*a* in different areas of the Gulf.
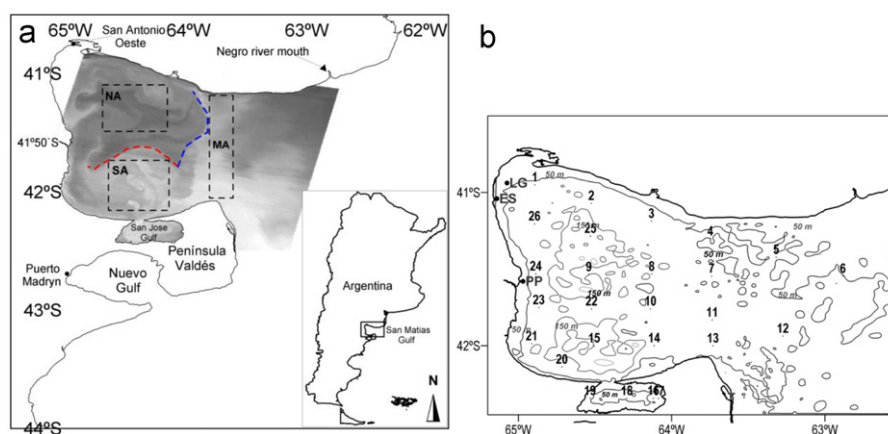
Fig. 1. (a) Study area and Landsat ETM+ brightness temperature image (March 8, 2004, adapted from Gagliardini and Rivas, 2004) showing the northern (warmer) and southern (colder) areas and the thermal fronts on the entrance (blue dashed line), and along 41°50′ (red dashed line) identified in previous studies. Northern, Southern and Mouth area (NA, SA, and MA, respectively) are also indicated. (b) General spatial distribution of *in-situ* data points (black points) on a bathymetric map. (For interpretation of the references to color in this figure legend, the reader is referred to the web version of this article.)

2. Material and methods

2.1. In-situ measurements

SST and chlorophyll-a data were collected during six research cruises (Table 1). Data of sea surface temperature were obtained from CTD profiles using a probe YSI 6600v2 (± 0.15 °C) and from a handheld multiparameter probe YSI 556 (± 0.15 °C) up to 5–10 m depth. Surface water samples were collected at each station (Fig. 1b). Chlorophyll-a was measured onboard by filtering 1 L samples through 47 mm Whatman GF/F filters. The filters were stored at -20 °C until analysis. Chlorophyll-a was extracted with 90% acetone and measured with a Turner Designs fluorometer according to Strickland and Parsons (1972).

In addition, records of sea surface temperature for the period 2005–2008 were obtained at three fixed coastal stations (Table 2), by an oceanographic buoy located approximately 3 km off the coast, in Las Grutas (LG), and two temperature data loggers (Optic Stow Away-Temp (°C) ONSET, ± 0.20 °C) in Punta Pozos (PP) and El Sótano (ES) (see locations in Fig. 1b) at 1 and 2.5 km from the coast, respectively. The temporal resolution of the oceanographic buoy and data loggers was 1 and 6 h, respectively, but daily averaged values at each site were available for comparison with satellite-derived values.

2.2. Remote sensing data

MODIS-Aqua spatially extracted Level-2 files were acquired for the study area (Fig. 1) from the NASA ocean color web page (http://oceancolor.gsfc.nasa.gov) for the dates with concurrent in-situ SST and Chl-a measurements. The standard Chl-a product derived from the OC3Mv5 algorithm (OC3M updated version after the 2009 reprocessing) and the daytime SST 11 μm product (which uses the 11 and 12 μm bands), were obtained. This SST product uses the standard MODIS 11 μm non-linear sea surface temperature (NLSST) algorithm with coefficients derived by the Rosenstiel School of Marine and Atmospheric Science (RSMAS) and input SST guess from Reynolds OISST product (http://www.cdc.noa.gov/cdc/data.reynolds_sst.html).

In order to define the temporal coincidence between satellite and in-situ measurements, different temporal windows were analyzed (± 3, ± 6, ± 12 and ± 24 h) and the ± 12 h window was selected in order to obtain a large number of match-ups within an acceptable temporal window. Available flags were used to assure the good quality of the retrieved product used in the comparison. For SST, only pixels with quality level less than two were used; "qual_sst" level ranges from zero (best quality) to four (complete failure) (Franz, 2006). For Chl-a products the following flags were used to mask unreliable retrievals: clouds, stray light on scenes, atmosphere correction, failure, high sun glint, observed radiance very high or saturated, high satellite and solar zenith angles, coccolithophores, and low normalized water-leaving radiance (Bailey and Werdell, 2006). Values of satellite SST and Chl-a used in the match-up were the median of all unmasked pixels within a 3×3 pixel box centered on the in-situ target; and satellite SST and Chl-a were excluded when more than 50% of marine pixels within this box were masked or when the coefficient of variation (ratio of the standard deviation to the mean) of the valid marine pixels exceeded 0.20.

The composite image for each cruise was generated to show the location of the match-ups and to have a general perspective of the SST, Chl-a, and cloud spatial distribution during each oceanographic cruise.

2.3. Testing MODIS standard SST and Chl-a algorithms

With the goal of evaluating the performance of the algorithms, linear regression analyses were carried out between the observed temperature and chlorophyll-a concentration, and the satellite products. The statistical parameters used for these evaluations were the mean relative percentage difference (RPD), the mean absolute percentage difference (APD) and the root mean square error (RMSE) between satellite-derived (sat) and measured (situ) SST and Chl-a, respectively. These parameters are defined as

$$RPD = \frac{1}{n} \sum_{n=1}^{N} ((X_{sat} - X_{situ})/X_{situ}) \times 100 \tag{1}$$

$$APD = \frac{1}{n} \sum_{n=1}^{N} |(X_{sat} - X_{situ})/X_{situ}| \times 100 \tag{2}$$

$$RMSE = \sqrt{\frac{1}{n} \sum_{n=1}^{N} ((X_{sat} - X_{situ})/X_{situ})^2 \times 100} \tag{3}$$

where X is the SST or Chl-a, and n is the number of match-ups analyzed. The slope, intercept and the determination coefficient (r_{SMA}^2) were calculated following a type II linear regression model, Standard Major Axis (SMA) (McArdle, 1988; Sokal and Rholf, 1995). Log transformations were applied to satellite and in-situ chlorophyll-a data since the bio-optical data have a log-normal distribution (Campbell, 1995). The linear-transformed root mean square error (RMSE-L) (Carder et al., 2004) and the root mean square log-error (RMSE_log), were calculated using the following equations:

$$RMSE-L = 0.5[(10^{+RMSE_{log}} - 1) + (1 - 10^{-RMSE_{log}})] \tag{4}$$

where

$$RMSE_{log} = \sqrt{\frac{1}{n} \sum_{n=1}^{N} (\log_{10}(Chl\text{-}a_{sat}) - \log_{10}(Chl\text{-}a_{situ}))^2} \tag{5}$$

Table 1
Research cruises for sampling in-situ data in San Matías Gulf. Date, season and number of data (n) are indicated.

Cruise name	Period	Season	n
GSM-I-07	23–27 June 2007	Autumn	25
GSM-II-02	17–19 October 2007	Spring	18
GSM-III-08	20–23 February 2008	Summer	26
GSM-IV-08	19–21 June 2008	Autumn	25
GMS-V-08	27–30 November 2008	Spring	23
GMS-VI-08	02–03 October 2009	Spring	17

Table 2
Location of temperature records in San Matias gulf. n: Number of records.

Place name	Latitude	Longitude	Date	n
Las Grutas (LG)	40°57′S	065°41′W	July 4–December 27, 2005	174
Punta Pozos (LP)	41°35′S	064°58′W	October 3, 2007–September 7, 2008	341
El Sotano (ES)	41°2′S	065°8′W	September 7, 2007–August 26, 2008	356

2.4. Analysis of the seasonal and spatial variability

In order to analyze the temporal variability of SST and Chl-a in the study area, monthly climatology composite images level-3 Global Area Coverage (GAC) MODIS SST and Chl-a data, corresponding to the period July 2002–May 2012 (nearly 10 years), were retrieved from the NASA ocean color web page (http://oceancolor.gsfc.nasa.gov/cgi/l3). It is a nominal 4 km resolution product processed with the NLSST (11 μm daytime) and OC3Mv5 (R 2009) algorithms. These data were sub-sampled over the study area (40°40′–42°23′S and 62°W–65°08′W) and re-gridded to a Geographic Lat/Long WGS 84 projection at $0.03331 \times 0.03331°$ resolution.

Mean and standard deviation temporal composites of SST and Chl-a were formed by arithmetically averaging all monthly climatology available scenes, on a pixel-by-pixel basis. Three areas were selected for the analysis (Fig. 1a) according to the characteristics described for SMG in previous works (Carreto et al., 1974b; Scasso and Piola, 1988; Rivas and Beier, 1990; Williams et al., 2010). Two areas were located within the SMG, the northern and southern regions (NA and SA, respectively); the third area covered the mouth of the gulf (MA). Time series of the whole gulf were also analyzed. The temporal variability of the monthly mean of SST and Chl-a values were extracted from each area. The SST stationary signal as well as the annual harmonics for each area, from 12 climatological monthly SST composites, were calculated using least square fitting (Beron-Vera and Ripa, 2000). Regardless of the semiannual component, the fit reduced to

$$SST(x,t) = SST_0(x) + T_1(x)\cos[w(t-t_0)] \tag{6}$$

where SST_0 is the mean SST temporal value, T_1 is the annual harmonic amplitude, w is the frequency ($w=2\pi/12$), and t_0 is the annual harmonic phase. In this case t_0 indicates the time of the year with maximum SST.

3. Results and discussion

3.1. Match-up analysis

The total number of in-situ data collected on the oceanographic cruises and fixed stations was 1005 for SST and 134 for Chl-a. Due to cloud cover, quality and the temporal coincidence criteria (± 12 h) used, the number of match-ups was reduced to 230 and 40 for SST and Chl-a, respectively. Thus, data from four (June and October 2007 and February and November 2008) of the six oceanographic cruises were represented in the analysis of comparison between satellite and in-situ data. These data covered a range of in-situ temperature and Chl-a values from 9.64 to 20.27 °C and 0.06 to 5.37 mg m^{-3}, respectively, while satellite-derived values ranged between 10.01–20.92 °C and 0.35–2.70 mg m^{-3}, respectively.

3.1.1. Sea surface temperature

The performance of MODIS–SST operational algorithm is presented for the data sets of each cruise and the fixed stations in Fig. 2 and Table 3. All linear correlations were statistically significant ($p < 0.05$) for each data set (oceanographic and fixed stations) except
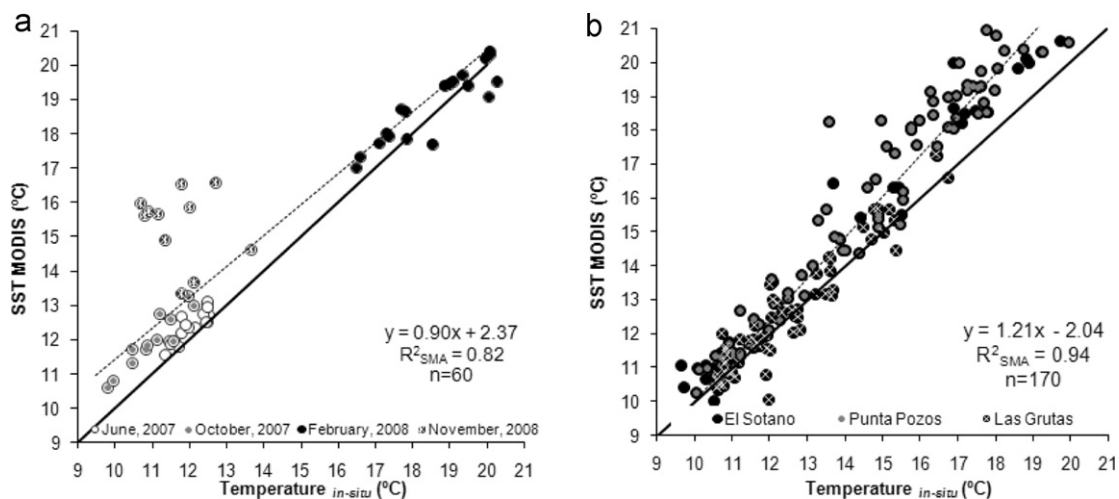
Fig. 2. Satellite-derived estimates *versus* measured sea surface temperature for (a) oceanographic cruises for different periods, and (b) the three fixed stations. The dotted line is the linear regression and the solid line represents the 1:1 relationship.

Table 3
Statistical results of the SST NLSST algorithm comparison.

Name	Slope	Intercept	n	r^2	p	RPD (%)	APD (%)	RMSE (%)
All data sets	1.11	−0.67	230	0.89	0.00	6.22	7.10	10.56
Winter (June 2007)	1.07	0.47	18	0.80	0.00*	2.81	2.93	3.37
Spring (October 2007)	1.12	−0.40	12	0.88	0.00*	7.90	8.63	8.95
Summer (February 2008)	0.83	3.45	19	0.81	0.00*	1.31	2.88	3.29
Spring (November 2008)	−1.17	29.36	11	0.04	0.54 ns	13.26	31.26	34.14
All cruises	0.90	2.37	60	0.82	0.00*	7.04	9.24	15.38
Pta. Pozos	1.21	−1.89	81	0.94	0.00*	7.98	7.17	8.60
El Sotano	1.10	−0.49	33	0.91	0.00*	6.34	6.33	7.21
Las Grutas	1.07	−0.76	56	0.89	0.00*	0.86	3.60	4.83
All fixed stations	1.21	−2.04	170	0.94	0.00*	5.31	6.34	8.19

* Statistically significant; ns: statistically non-significant; $p < 0.05$.

for November 2008. The mean absolute percentage difference (APD) of the data set ranged between 2.88% and 8.63%, the mean relative percentage difference (RPD) varied from 1.31% to 7.98% while the root mean square error (RMSE) varied between 3.29% and 10.56% except for November 2008 for which the APD, RPD and RSME were 31.26%, 13.26% and 34.14%, respectively, indicating more uncertainty and a positive bias. The high dispersion in the November 2008 data set may be attributed to a malfunction of the handheld probe. The average of *in-situ* values was $11.7 \pm 0.9 \,^{\circ}\text{C}$ (with minimum and maximum of $10.7 \,^{\circ}\text{C}$ and $13.7 \,^{\circ}\text{C}$, respectively), much lower than the SST value estimated by MODIS sensor ($15.3 \pm 1.1 \,^{\circ}\text{C}$). *In situ* SST match-ups were within the range obtained from the MODIS–SST time series extracted from Ocean Color web (http://oceancolor.gsfc.nasa.gov/cgi/l3) for the SMG area in November 2008 (November 2008 presented an average SST value of $13.8 \pm 1.1 \,^{\circ}\text{C}$, with minimum and maximum of $11.4 \,^{\circ}\text{C}$ and $17.8 \,^{\circ}\text{C}$, respectively). Also, the average SST for November 2008 was consistent with the climatological value for the 2002–2011 period ($13.4 \pm 1.0 \,^{\circ}\text{C}$, with minimum and maximum of $10.5 \,^{\circ}\text{C}$ and $18.7 \,^{\circ}\text{C}$, respectively).

The fit of the temperature data to a SMA type II regression model indicated that a high proportion of the total variance ($r^2 \geq 0.80$) was explained by the model for each oceanographic cruise and fixed station (Table 3). In general, the regression analysis considering all data conforms well to the SST–MODIS estimates. The APD, RPD and RMSE values were 6.22%, 7.10% and 10.56% respectively, indicating relatively low uncertainty and a positive bias. The slope was close to one with a negative intercept (-0.67). The correlation coefficient indicated that 89% of the total variance was explained by the SMA model for all the data (Table 3). These results are in agreement with those obtained in the comparison with AVHRR-SST data for records obtained in June and October of 2007 (Williams et al., 2010) which also showed high correlation and overestimation of the *in-situ* values.

The maps corresponding to June and October 2007 and October 2009 (in 2009 match-ups were not obtained) show low SST with a uniform distribution (12–13 °C) over the gulf; however relatively lower temperatures around Peninsula Valdés were also observed (~ 10 °C) (Fig. 3). The SST map of February 2008 shows warmer temperatures (16–22 °C); the temperature in the inner area of the gulf was higher (22 °C) than that in the mouth. It was not possible to observe the SST spatial distribution for June and November 2008 due to high cloudiness in the area (Fig. 3b, d).
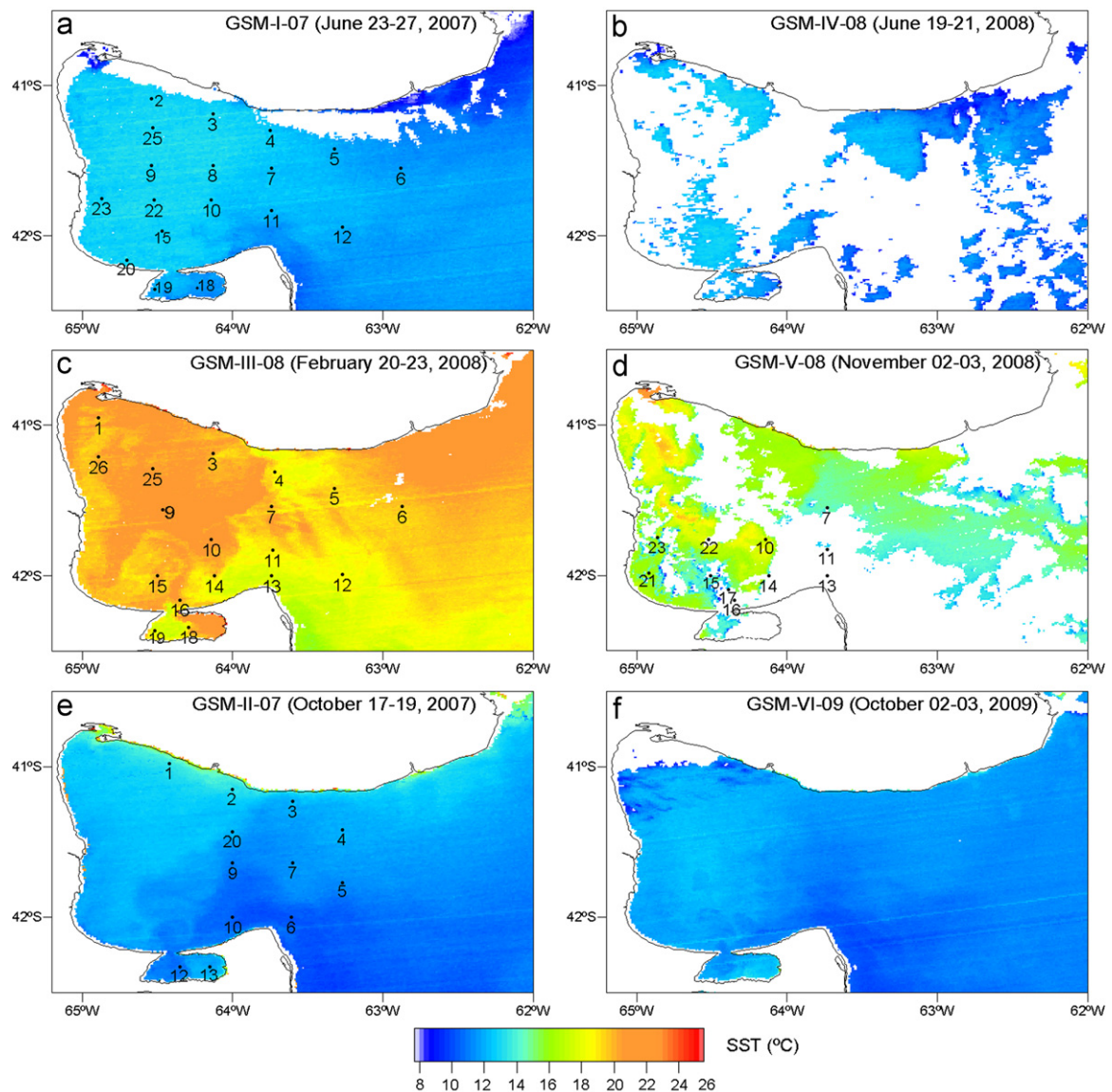
Fig. 3. MODIS SST composite maps for cruises of June—2007 (a), June—2008 (b), February—2008 (c), November—2008 (d), October—2007 (e) and October—2009 (f). The numbers indicate the location of match-ups for each oceanographic cruise.
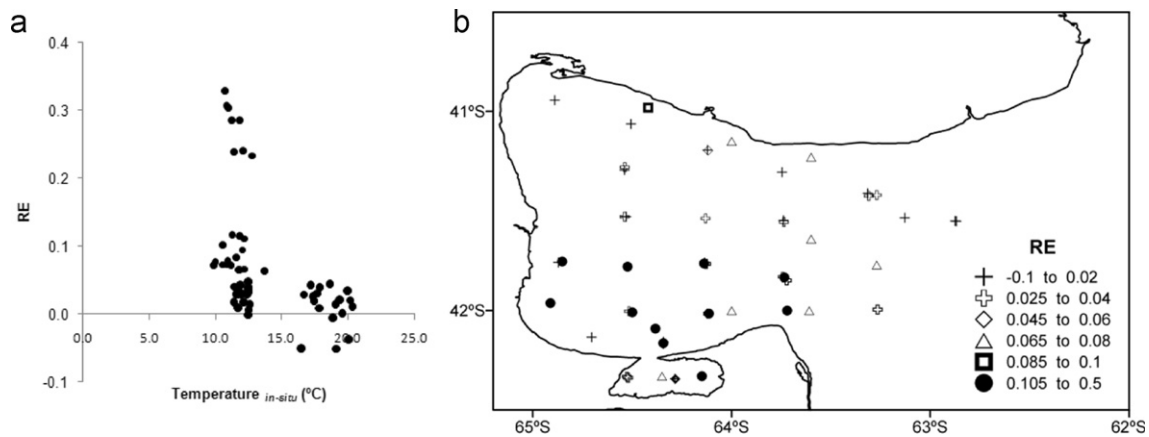
Fig. 4. MODIS SST (NLSST algorithm) relative error, sat-*situ*: (a) *versus in situ* SST (*n*=60) and (b) spatial distribution in the SMG.
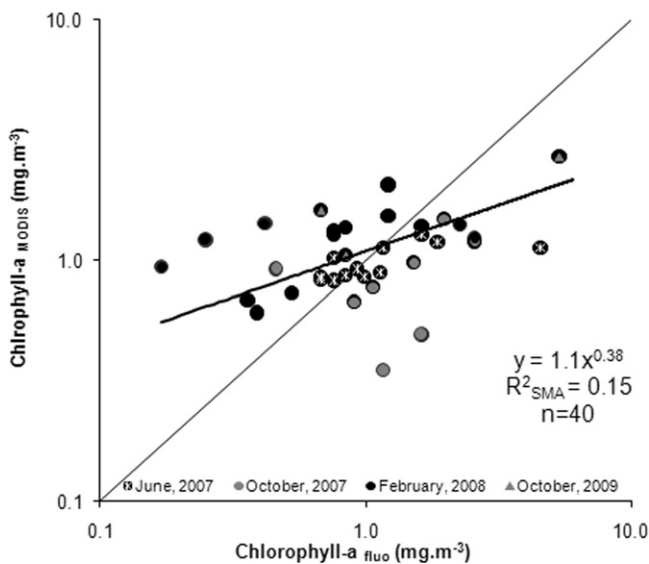
Fig. 5. Satellite-derived *versus* measured Chl-*a* for all data sets. The bold line is the linear regression and the thin line represents the 1:1 relationship.

These results show a high correlation between both satellite and *in-situ* data; however, satellite-derived SST generally overestimated *in-situ* records as indicated by the positive RE (Fig. 4a) and its spatial distribution showed that the highest RE tended to occur in the southern part of GSM (Fig. 4b). NLSST algorithm was developed using SST data from buoys located mainly in the Northern Hemisphere, so the average error of 0.05 °C indicated for MODIS–SST estimates is only nominal for those latitudes and may not be representative of the average atmospheric conditions of the study area (Brown and Minnett, 1999). On the other hand, the use of daily average sea surface temperature records from fixed stations and the temporal window of 12 h could result in an overestimation and a higher scatter of data in the regression models presented. It has been observed that nighttime SST products correlated most favorably with *in-situ* buoy SSTs (Montgomery and Strong, 1995), thus the use of only nighttime observations attempts to minimize the effects of diurnal variation. Indeed, in this work, daytime images were used from MODIS sensor (in order to obtain simultaneously images of chlorophyll-*a*), which in principle could explain the overestimation of *in-situ* records.

3.1.2. Chlorophyll-a concentration

The regression analysis for chlorophyll-*a* considering all matchups shows low correlation coefficients (r^2=0.15, Fig. 5 and Table 4). The statistical parameters indicate a poor performance of the empirical algorithm over the SMG with a general overestimation of Chl-*a* by MODIS sensor with respect to fluorometric data, as shown by the positive RPD (Table 4). The ratio of satellite to *in-situ* measurements for two *in-situ* Chl-*a* ranges showed that for concentrations less than 1.0 mg m^{-3}, OC3Mv5 algorithm tends to overestimate Chl-*a* in relation to *in-situ* measurements, and that at concentrations greater than 1.0 mg m^{-3}, it tends to underestimate it (Table 5). The plot of the relative error (RE) as a function of the *in-situ* Chl-*a* range clearly shows a general decrease in the algorithm performance for concentrations higher and lower than 1.0 mg m^{-3} and a change of sign in the RE around 1.0 mg m^{-3} (Fig. 6a), in agreement with previous observed bias (Dogliotti et al., 2009). Also, the RE showed higher values in the southern sector of the Gulf (Fig. 6b). Moreover, the change of sign in the RE around 1.0 mg m^{-3} can be clearly observed in the *in-situ* records, coincidently with the previously observed bias (Fig. 6a). Similar results were obtained using the data set from June and October 2007 for SeaWiFS OC4v.4 algorithm (Williams et al., 2010).

Statistical analyses grouping the data by season show significant linear correlations and improved results are obtained (Table 4), except for the summer cruise (February 2008) which shows the highest RPD, APD, RMSE-log and RMSE-L (229.48%, 242.71%, 0.50 and 1.44, respectively) compared to the other data sets analyzed. It is worth mentioning that the number of matchups is relatively lower when a seasonal analysis is performed. In spring, the RPD indicates an underestimation of *in-situ* chlorophyll-*a* by OC3Mv5 algorithm and an uncertainty of 56% (Table 4). The analysis of data sets with a significant correlation shows that June 2007 has the highest correlation coefficient (r^2=0.61), but the lower slope (0.19) and a relatively high and positive bias in Chl-*a* values, as estimated by de RPD of 72.19% (Table 4).

As previously mentioned, the underestimation at concentrations higher than 1.0 mg m^{-3} occurred mainly in spring (gray points and triangles in Fig. 5), and could be related with the presence of chain-forming diatoms species that may influence the optical properties of the water (Stuart et al., 1998). In this study it was not possible to get data on phytoplankton composition; however the structure and distribution of the phytoplankton community in SMG during winter, spring and summer of 1993, 1992 and 1994, respectively, were dominated by diatoms and silico-flagellates (Sastre et al.,1997). Among diatoms these authors identified the chain-forming species like *Chaetoceros* spp. and *Thalassiosira* spp.
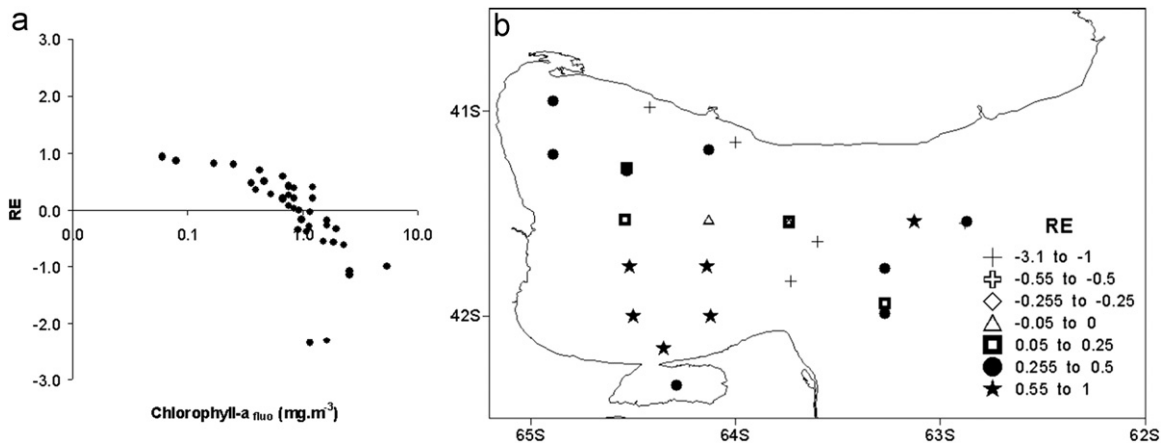
Fig. 6. MODIS Chl-a (OC3M algorithm) relative error (sat-situ): (a) *versus in situ* Chl-a and (b) spatial distribution in the SMG.

Table 4
Statistical results of the Chl-a OC3Mv5 algorithm comparison.

Season	Slope	Intercept	n	r^2	p	RPD (%)	APD (%)	RMSE-log	RMSE-L
All cruises	0.38	0.04	40	0.15	0.01*	112.88	144.73	0.41	1.09
Winter (June 2007)	0.19	−0.02	13	0.61	0.00*	72.19	99.00	0.35	0.89
Summer (February 2008)	0.34	0.13	16	0.36	0.01*	229.48	242.71	0.50	1.44
Spring (October 2007 and 2009)	0.84	−0.12	11	0.17	0.20 ns	−8.65	56.26	0.31	0.78

* Statistically significant ($p < 0.05$); ns: not significant.

Table 5
Ratio (mean ± standard deviation) of satellite-derived to *in-situ* Chl-a values.

	Chl-a$_{fluo}$ < 1.0 mg m^{-3}	Chl-a$_{fluo}$ > 1.0 mg m^{-3}
Mean	3.18	0.70
SD	3.86	0.36
N	23	17

If a similar phytoplankton community structure were present in the cruises analyzed in the present study, the underestimation could be explained by a decrease in the specific absorption coefficient of phytoplankton (*i.e.* the absorption coefficient of phytoplankton per unit of Chl-a) due to the particle effect (also known as the "package effect") when large-size cells are present (Sathyendranath et al., 2001). This effect theoretically predicts the flattening of the absorption spectra (*i.e.* a decrease of the absorption efficiency) with increasing cell size and pigment concentrations (Duysens, 1956; Sathyendranath et al., 1987).

Concentrations of chlorophyll-a lower than 1.0 mg m^{-3} were identified mainly in summer (February 2008; black symbols in Fig. 5). Carreto et al. (1974a, 1974b) and Sastre et al. (1997) also found that dinoflagellates dominated some samples of the northwestern sector mainly in spring. However, for summer, the historical analysis of the phytoplankton community did not allow us to interpret the overestimation of the *in-situ* values. Therefore it is necessary to monitor the phytoplankton community and the concentration of Chl-a jointly with other bio-optical and environmental variables (for example, the stability of the water column) to validate this hypothesis. Lutz et al. (2006) observed that hydrographic characteristics and changes in the phytoplankton community structure significantly affect the satellite-derive Chl-a estimates in a nearby region.

Finally, for concentrations close to 1.0 mg m^{-3} the scatterplot shows less bias in the *in-situ* and satellite values. This situation was clear in winter (June 2007) when surface distributions of SST and Chl-a were more uniform.

The general overestimation of Chl-a in the whole region could be related to the presence of other optically active components than Chl-a, such as colored dissolved organic matter (CDOM) or sediments that may cause the blue to green reflectance ratio algorithms to return biased values. Many of the match-ups with high RE (Fig. 6b) were located in the southern part and mouth of the gulf and might be affected by sediments re-suspension. It has been observed that the accuracy of the OC4v4 (SeaWiFS) and OC3Mv5 (MODIS) algorithms retrieval generally degraded with increasing optical complexity in more coastal waters. In particular, the OC3Mv5 algorithm from MODIS sensor overestimated *in-situ* measurements by 40–100% (Werdell et al., 2009).

Composite Chl-a maps corresponding to June 2007 and February 2008 show low and uniform Chl-a distribution in the inner area (≤ 1.0 mg m^{-3}) and higher concentrations were observed in the mouth of the gulf (Fig. 6). In October 2007 and 2009 high concentration patches were observed in the northern area of the mouth, around Peninsula Valdés, in the southwest and outer areas. In June and November 2008 it was not possible to observe the Chl-a distribution due to high cloud cover area (Fig. 7b, d). In relation to these observations a tidal front has been identified in the mouth of SMG (Glorioso and Simpson, 1994; Rivas and Dell'Arciprete, 2000; Gagliardini and Rivas, 2004; Tonini et al., 2007; Williams et al., 2010) being the tidal energy flow in this area very important (Tonini et al., 2007). The Simpson–Hunter criterion computed from model results (Palma et al., 2004) indicated vertical mixing zones on the mouth of SMG which coincides with the local distribution of non-case 1-waters previously determined in this region (Dogliotti et al., 2009). In the MA of the gulf the high tidal energy flow could cause the resuspension of bottom sediments while the Negro river discharge on the northeast coast of SMG could contribute with particulate and dissolved detritus material of terrestrial origin. The standard atmospheric correction algorithm that was used in the L2
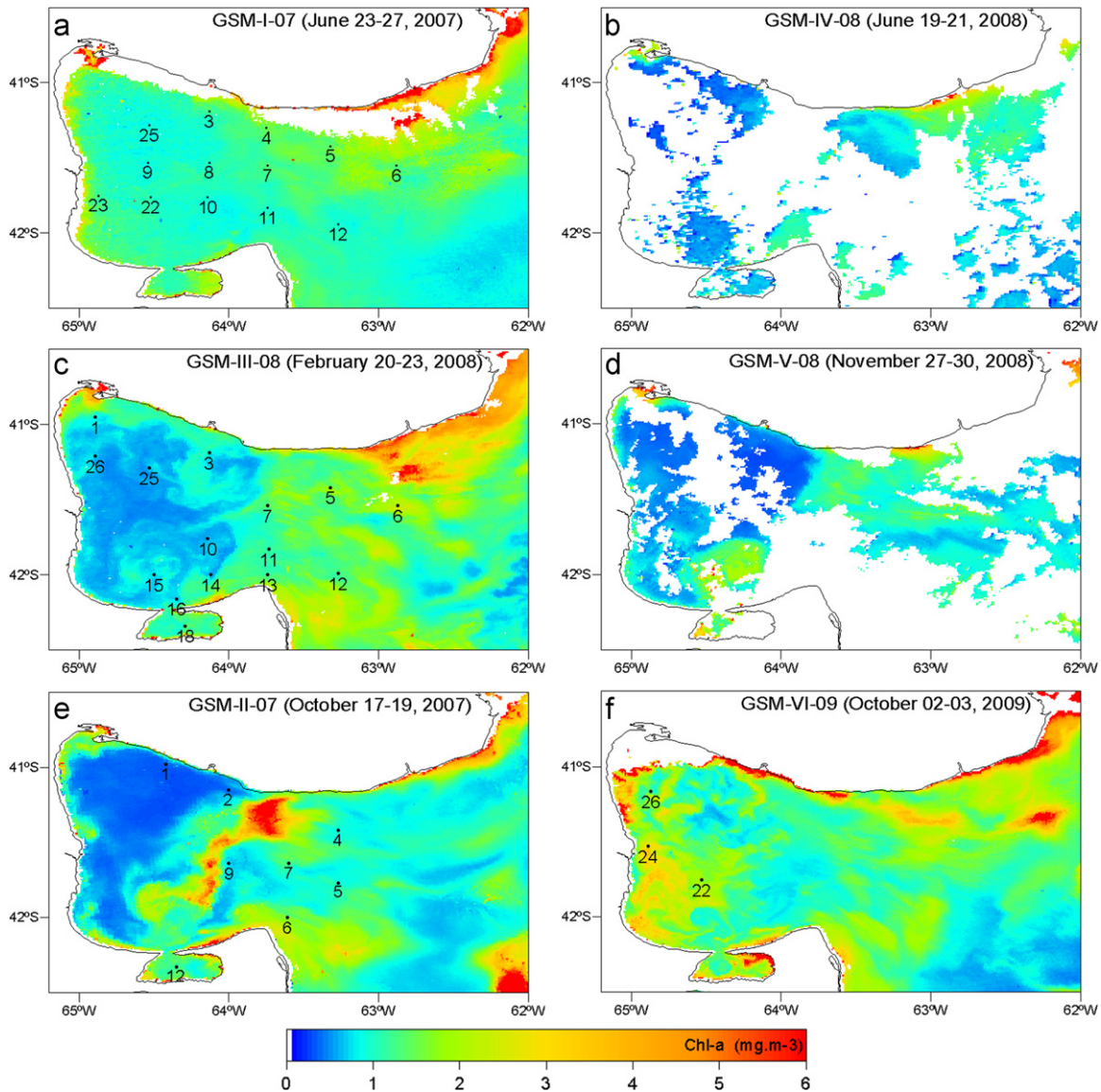
Fig. 7. MODIS Chl-*a* composite maps for the cruises of June—2007 (a), June—2008 (b), February—2008 (c), November—2008 (d), October—2007 (e) and October—2009 (f). The numbers indicate the location of the match-ups for each oceanographic cruise.

processing of the images used relies on the assumption of negligible water-leaving reflectance in the near-infrared (NIR) region of the spectrum for the open ocean with modifications to account for the water-leaving reflectance contribution in the NIR bands for more coastal moderately turbid or highly productive waters (Stumpf et al., 2003; Bailey et al., 2010). Therefore, if the amount of re-suspended sediments is relatively high, the estimation of the marine contribution in the NIR might not be correct. Problems with the atmospheric correction performance could also be related to the global aerosol model used in the processing (available in the SeaDAS software) compared to the local aerosol type found in the region. Close to the study region there was an AERONET (AErosol RObotic NETwork) station located in Puerto Madryn (42.8°S 65.0°W) which collected data from June 2000 to July 2003 and another station, 60 km south of Puerto Madryn (Trelew: 43.2°S 65.3°W), which has been collecting data since November 2005. The evolution of the aerosol optical thickness (τ) at Puerto Madryn station during 2002 showed that the aerosol types found were mainly Maritime with high salt content and Antarctic (with similar characteristics to Maritime regarding the Angstrom and τ(440 nm) values) with

salts and sulfates, and also presented aerosols from industrial sources, dust, salt and sand (Otero et al., 2006). A new set of aerosol models has been developed and implemented in the sixth reprocessing of the MODIS mission (R2009) using AERONET retrievals as a guide to use realistic range of optical properties from which to simulate the model suite (Ahmad et al., 2010). Even though none of the stations in our study region were included in this analysis, it included a site in Chesapeake Bay Region (CBR) where the aerosols are influenced by industrial and city pollutions, agricultural land use, and the Atlantic Ocean, thus we expect that the models currently used could be applicable in this region, except for the presence of dust. Dust emission events from the Patagonian desert to the South Atlantic Ocean are known to occur and have been previously reported (Gaiero et al., 2003; Gasso and Stein, 2007). Moreover, a dust event recorded on March 28, 2009 was analyzed using information from the AERONET station located in Trelew and it was characterized as Dust with single scattering albedo of 0.9 and τ_{440} of 0.8 (Otero et al., 2009). In the present study and for the match-up stations values of τ_{869} varied between 0.0042 to 0.1642 evidencing clear atmospheric

conditions (≤ 0.2), therefore no evidence of the presence of a dust plume was found during the sampling dates.

An additional source of error may be the uncertainty in the *in-situ* measurements. The fluorometric technique used in this work is known to have high sensitivity to detected chlorophyll-*a* concentration but has less precision than the spectrophotometric method (Strickland and Parsons, 1972). The accuracy depends strongly on the concentration of pigment to be determined, being less than 8% for Chl-*a* values exceeding 0.5 mg m^{-3} (Strickland and Parsons, 1972). However, *in-situ* concentration of Chl-*a* in the samples ranged between 0.06 and 5.37 mg m^{-3}, and 77% of all data analyzed were higher than 0.5 mg m^{-3} above which the sensitivity of the method can be considered adequate.

The peculiar characteristics of the SMG may partially explain the observed performance of the empirical algorithms in this region. As mentioned before, many of the data used in the analysis were located near the shore or the mouth of the gulf, and therefore are affected by the high tidal energy flow. Even though no optical data are available to support this hypothesis, the mouth of SMG can be characterized as non-case 1-waters (Dogliotti et al., 2009), where empirical case 1-water algorithms are known to fail.

Based on the particular characteristics of the mouth and the southern area of SMG (shallow, intense tidal currents, tidal front presence and high levels of energy dissipation), only stations located in the northern area of the gulf were selected for a new analysis. The reduced data set showed a higher correlation ($r^2 = 0.76$) and lower APD, RPD, RMSE$_{log}$ and rmse-L (30.55%,

30.77%, 0.14, and 0.09, respectively) compared to data sets previously analyzed, even though the slope did not exceed 0.50 (Fig. 8). The better results found with this data set could be related to the isolated nature of the northern area of the gulf, *i.e.* low renewal rate (Rivas and Beier, 1990), low sediment concentration due to the lack of river run-off, high depths and deep seasonal thermocline (> 100 m). The results found in the present work are in agreement with the typical uncertainty of global algorithms when applied to regional scales (Szeto et al., 2011), emphasizing the need of regional data sets in order to take into account local variability of the bio-optical properties.

3.2. Seasonal and spatial variability of SST and Chl-a—sat

Spatial distribution of the temporal mean of SST shows the input of cold water on the south of the MA, as well as the isolation of the northern area from the continental shelf. The average monthly values registered at each point permitted to identify the influence that water dynamics has on the spatial distribution of SST (Fig. 9a). Variability associated to the mean temporal value is mostly due to the annual signal, as it will be shown later (Fig. 9b). The northwestern area of the gulf was characterized by average chlorophyll-*a* concentrations below 1.0 mg m^{-3} (Fig. 10a). The area of the mouth, the outer zone of the north coast (close Negro river) reported the highest average concentrations of Chl-*a* (2.0–3.0 mg m^{-3}) (Fig. 10b). These maps show that SMG can be separated into two regions according to SST and Chl-*a* distribution. One is the northwest, characterized by the highest average values of
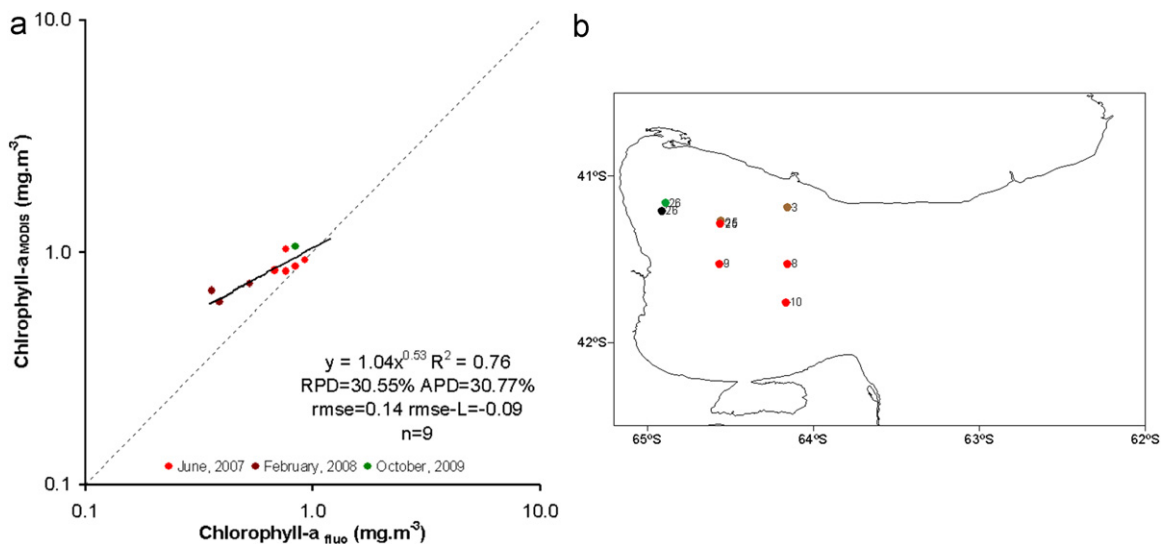
Fig. 8. (a) Satellite-derived *versus* measured Chl-*a* for match-ups located at depths greater than 50 m within the gulf, *i.e.* in the center of the northern area. (b) Map showing the location of the match-ups. The solid line is the linear regression and the dotted line represents the 1:1 relationship.
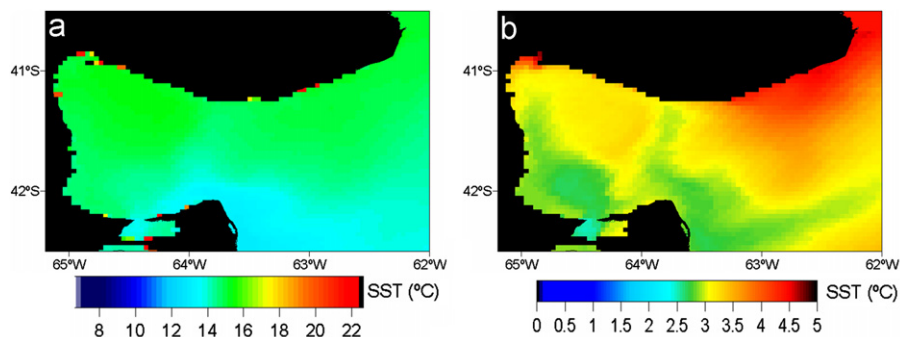
Fig. 9. Spatial distribution of the temporal mean of SST (a), and its corresponding standard deviation (b).
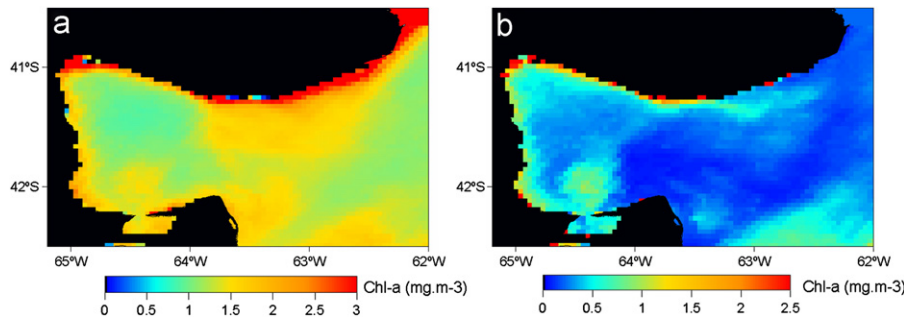
Fig. 10. Spatial distribution of the temporal mean of Chl-*a* (a), and its corresponding standard deviation (b).
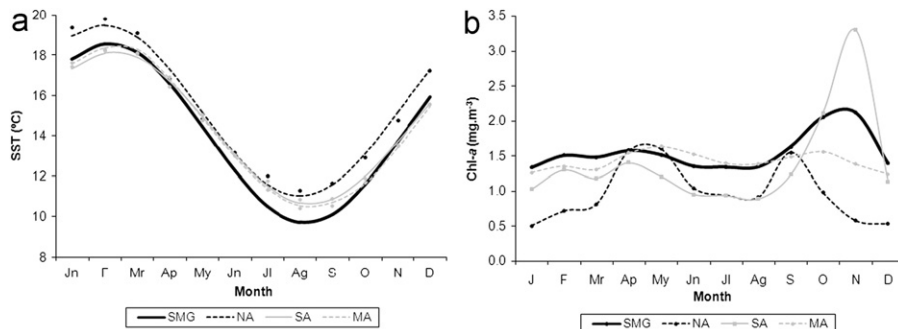
Fig. 11. Mean annual cycle of MODIS (a) SST and (b) Chl-*a* monthly mean values at each area for the period 2003–2009.

Table 6

Results of MODIS SST time series analysis. Mean temporal value (SST_0), annual harmonic amplitude (T_1), frequency (W), annual harmonic phase (t_0), and correlation coefficient (r^2). Location of the Northern, Southern and Mouth Areas (NA, SA and MA, respectively) are shown in Fig. 1.

Area	SST_0	T_1	w	t_0	r^2	Min. obs.	Max. obs.
GSM	14.14	4.43	0.52	2.13	0.9984	9.90	18.72
Northern area (NA)	15.25	4.25	0.52	1.96	0.9947	11.27	19.82
Southern area (SA)	14.39	3.76	0.52	2.28	0.9974	10.85	18.24
Mouth area (MA)	14.34	4.01	0.52	2.33	0.9990	10.54	18.36

Table 7

Results of MODIS Chl-*a* time series analysis for each area (see Fig. 1).

Area	Mean	Max	Min	SD	Month of max.	Month of min.
GSM	1.55	2.11	1.34	0.27	November	July–August
NA	0.98	1.60	0.50	0.40	March	January
SA	1.39	3.29	0.89	0.68	November	August
MA	1.42	1.63	1.24	0.13	March	December–January

SST (17.0 °C ± 3.5 °C), and low Chl-*a* concentrations ($\sim$1.0 mg m^{-3}) throughout the year. The other regions, the southern area, the mouth of the gulf and the shelf (external region) were characterized by high concentrations ($>$1.0 mg m^{-3}) and lowest SST average values (16.0 °C ± 2.5 °C).

The climatologically monthly SST data ranged between 9.90 and 18.72 °C; 11.27 and 19.82 °C; 10.85 and 18.24 °C; and 10.54 and 18.36 °C for SMG, NA, SA and MA, respectively, in the time series analyzed (Fig. 11a and Table 6). The amplitude (T_1), phase (t_0) and percentages of the variance explained by the annual harmonic (r^2) for the thermal cycle at each area are shown in Table 6. The marked annual signal is evidenced by the high percentage of the explained variance ($r^2 > 0.99$). The NA of the gulf had the highest mean temperature (15.25 °C) and amplitude (4.25 °C). The MA had the lowest minimum and mean temperature (10.54 and 14.34 °C, respectively) and the SA had the lowest amplitude (3.76 °C) (Fig. 11a and Table 6). Moreover, the thermal cycles of the analyzed areas present different SST between August and April being the SST of the NA always higher than the remaining areas, while in May and June the average SST was similar (Fig. 11a). The average SST of the SA and MA were lower than SMG and NA between November and March. Also, the average temperature of the MA was slightly higher than the SA from January to March and lower from August to November.

The annual cycle of Chl-*a* for the whole SMG (black line, Fig.11b) showed relatively higher concentrations of Chl-*a* with respect to the NA and SA areas (1.55 ± 0.27 mg m^{-3}, Fig. 11b, Table 7), with one peak in November (spring bloom). The northern area (black dashed line in Fig. 11b) presents a mean concentration of 0.98 ± 0.40 mg m^{-3} and two peaks, one in fall months (April–May) and the other in spring (September). The SA (gray line, Fig. 11b) presents a mean concentration of 1.39 ± 0.68 mg m^{-3} and one peak in spring (November), with relative higher values than the NA between October and March. The mouth of the SMG (gray dashed line, Fig. 11b) shows mean concentrations of 1.42 ± 0.13 mg m^{-3} with relatively low annual variation.

The parameters for the annual cycles in each area help us to explain the annual variability in the concentration of Chl-*a*: the annual harmonic phase of SST (Table 6), that indicates the time of the year with maximum SST, tended to be lower (earlier in the year) in the northern area ($t_0 = 2.13$, early February) compared to the southern, indicating a higher trend to seasonal stratification. In general, the annual harmonic phase of SST is higher in zones that do stratify seasonally, where summer heat flux is distributed over the upper layer of the water column and thus the maximum temperature is reached earlier than in zones where mixing keeps the water column homogeneous (Rivas, 2010). The minimum value of Chl-*a* (0.50 mg m^{-3}, Fig. 11b) recorded in January, could be explained by the stratification of the water column (Rivas and Beier, 1990; Williams, 2004) and consumption of phytoplankton by bivalve beds (mainly mussels, clams, scallops and oysters;

Morsán, 2003; Narvarte et al., 2007). Thus, the Chl-*a* cycle in the northwestern area presents a spring bloom limited by nutrients (due to stratification) and a subsidiary bloom in autumn caused by the decrease of temperature in the surface layer and the subsequent mixing of the water column. The northern and western areas have been identified as areas of high temperature and salinity, with a marked thermocline and a low renewal rate (Carreto et al., 1974a, 1974b; Rivas and Beier, 1990; Gagliardini and Rivas, 2004; Williams, 2004; Tonini et al., 2006).

The southern area showed higher Chl-*a* values than the northern region in spring and summer. The minimum Chl-*a* value in the southern area was recorded in August ($\sim$0.89 mg m^{-3}) and could be related to the low light availability (Greenan et al., 2004). In this area Chl-*a* increased in spring and continued high in summer probably sustained by the upwelling of nutrients caused by the interaction of tidal currents with the topography. The annual harmonic phase of SST annual cycle was relatively higher in this sector ($t_0 = 2.28$, mid-February) indicating a lower trend to stratification.

The relatively high concentrations in the MA may result from the high tidal energy flow that prevents the stratification of the water column. The high concentrations of Chl-*a* detected by the sensor could be either an artifact, resulting from the presence of sediments from the Negro river discharge, or otherwise, it could be caused by the actual presence of phytoplankton, favored by the availability of nutrients. The analysis of the thermal cycle in the MA (Table 6) showed that the annual harmonic phase was the highest ($t_0 = 2.33$), indicating that this area has a thermal cycle typical of shallow and mixed waters according to the presence of the tidal front in the mouth of the SMG (Palma et al., 2004; Tonini et al., 2007). The southern and south-eastern areas of SMG have been identified as areas with low temperature and salinity, lack of stratification, and strongly influenced by the intrusion of cold water from the south (Carreto et al., 1974a, 1974b; Rivas and Beier, 1990; Gagliardini and Rivas, 2004; Williams, 2004; Tonini et al., 2006).

These results show that the thermal cycles calculated using SST data from the MODIS sensor were in agreement with previous studies (Carreto et al., 1974a, 1974b; Rivas and Beier, 1990; Gagliardini and Rivas, 2004). The seasonal variability of the mean Chl-*a* over the whole area of SMG can be summarized as follows: average concentrations range between 1.34 and 2.11 mg m^{-3}, minimum values between December and August ($\sim$1.30 mg m^{-3}), and high concentrations in November. This seasonal cycle is typical of subtropical waters where the rate of primary production is relatively stable in autumn–winter and peaks in late spring before nutrients became limiting again. In summer phytoplankton biomass does not reflect the peak in primary production, probably because it is removed by zooplankton grazing (Mann and Lazier, 1996). So, the analysis of the different sub-areas of the gulf showed differences in the Chl-*a* variability according to the particular characteristics of each area: seasonal stratification, influence from continental shelf and bottom topography.

4. Summary and conclusions

This paper illustrates the application of remote sensing data to the analysis of a coastal water ecosystem. Attention has been focused on two parameters useful for describing the status of the ecosystem and commonly retrieved from remotely sensed data: sea surface temperature and chlorophyll-*a* concentration.

A good fit between the remotely sensed SST and the temperature records over the whole investigated area was observed, however the NLSST algorithm slightly overestimated *in-situ* records.

In this paper, uncertainties in the retrieval of MODIS-derived surface Chl-*a* concentration have been evaluated in SMG for the first time. A systematic error was found in the satellite-derived Chl-*a* for all the data sets analyzed, showing a general overestimation. A poor agreement was found when all the satellite-derived chlorophyll-*a* data for the study area are compared with the corresponding *in-situ* observations. The results presented in this paper suggest that in regions with high tidal dissipation the OC3Mv5 algorithm does not provide a good estimation of the chlorophyll-*a* concentration measured *in-situ*. The seasonal analysis of the available data set showed that the algorithm generally underestimated *in-situ* chlorophyll-*a* in the spring, while in winter and summer there was a general overestimation. These differences could be related to different environmental and biological characteristics present in each season (phytoplankton community structure, pigment composition, CDOM, *etc.*).

Regarding the satellite Chl-*a* estimations, the results suggest that MODIS data should be used carefully in the SMG. However, the analysis of its seasonal variability was coincident with previous studies (Carreto and Verona, 1974b) as well as the thermal cycle in the main areas identified in SMG.

It would be useful to gather information on bio-optical properties as well as the taxonomic composition and cell abundance, in coincidence with the match-ups, since it would help understand and partially explain the differences found between *in-situ* and satellite-derived values. For a more comprehensive analysis, a larger dataset of bio-optical *in-situ* measurements is clearly necessary in order to perform an analysis based on the first principles of ocean color (Sathyendranath et al., 2001), as well as *in situ* reflectance measurements to assess the atmospheric correction algorithm performance. The results of this study show that despite the absolute differences between satellite and *in-situ* data, the temporal variability observed by remote sensors reproduces known patterns.

References

Ahmad, Z., Franz, B.A., McClain, C.R., Kwiatkowska, E.J., Werdell, J., Shettle, E.P., Holben, B.N., 2010. New aerosol models for the retrieval of aerosol optical thickness normalized water-leaving radiances from the SeaWIFS and MODIS sensors over coastal regions and open oceans. Applied Optics 49 (29), 5545–5560.

Bailey, S., Werdell, P., 2006. A multi-sensor approach for the on-orbit valitadion of ocean colour satellite data products. Remote Sensing of Environment 102, 12–23.

Bailey, S.W., Franz, B.A., Werdell, P.J., 2010. Estimation of near-infrared water-leaving reflectance for satellite ocean color data processing. Optics Express 18 (7), 7521–7527.

Bailey, S.W., McClain, C.R., Wedell, P.J., Schieber, B.D., 2000. Normalized water-leaving radiance and chlorophyll-a match-up analyses. In: Hooker, S.B., Firestone, E.R. (Eds.), SeaWiFS Postlaunch Technical Report Series, 10, SeaWiFS Postlaunch Calibration and Validation Analyses, Part 2. NASA Technical Memorandom 2000-206892, 10. NASA/Goddard Space Flight Center, Greenbelt, MD, pp. 45–52.

Barré, N., Provost, C., Saraceno, M., 2006. Spatial and temporal scales of the Brazil-Malvinas Current confluence documented by simultaneous MODIS Aqua 1.1-km resolution SST and color images. Advances in Space Research 37, 770–786.

Bava, J., 2004. Metodologías de procesamiento de imágenes NOAA-AVHRR y su utilización en aplicaciones oceanográficas y biológico-pesqueras en el

Atlántico Sudoccidental. Ph.D. Thesis. Universidad Nacional de Buenos Aires, Ciudad Autónoma de Buenos Aires, 142 pp.

Bava, J., Gagliardini, D.A., Dogliotti, A.I., Lasta, C.A., 2002. Annual distribution and variability of remotely sensed sea surface temperature fronts in the South-western Atlantic Ocean. In: Proceedings of the 29th International Symposium on Remote Sensing of the Environment. International Society for Remote Sensing of the Environment, Buenos Aires, Argentina, April 2002, pp. 8–12.

Behrenfeld, M.J., Falkowski, P.G., 1997. Photosynthetic rates derived from satellite based chlorophyll concentration. Limnology and Oceanography 42, 1–20.

Beron-Vera, F.J., Ripa, P., 2000. Three-dimensional aspect of the seasonal heat balance in the Gulf of California. Journal of Geophysical Research 105 (C5), 11441–11457.

Brown, O.B., Minnett, P.J., 1999. MODIS Infrared Sea Surface Temperature Algorithm Theoretical Basis Document, Version 2.0 [on line]. Available from: ⟨http://modis.gsfc.nasa.gov/data/atbd/atbd_mod25.pdf⟩.

Campbell, J.W., 1995. The lognormal distribution as a model for bio-optical variability in the sea. Journal of Geophysical Research 100, 13237–13254.

Carder, K.L., Chen, F.R., Cannizzaro, J.P., Campbell, J.W., Mitchell, B.G., 2004. Performance of the MODIS semi-analytical ocean color algorithm for chlorophyll-a. Advances in Space Research 33, 1152–1159.

Carreto, J.I., Verona, C.A., Casal, A.B., Laborde, M.A., 1974a. Fitoplancton, pigmentos y condiciones ecológicas del Golfo San Matías: II, Noviembre de 1971. Anales Informes Comisión de Investigaciones Científicas Provincia de Buenos Aires (La Plata), 10, 76 pp.

Carreto, J.I., Verona, C.A., 1974b. Fitoplancton, pigmentos y condiciones ecológicas del Golfo San Matías: I, Marzo de 1971. Anales Informes Comisión de Investigaciones Científicas Provincia de Buenos Aires (La Plata), 1–20.

Dogliotti, A.I., Shloss, I.R., Almandoz, G.O., Gagliardini, D.A., 2009. Evaluation of SeaWiFS and MODIS chlorophyll-a products in the Argentinean Patagonian Continental Shelf (38°S–55°S). International Journal of Remote Sensing 30 (1), 251–273.

Duysens, L.M.N., 1956. The flattening effect of the absorption spectra of suspensions as compared to that of solutions. Biochimica et Biophysica Acta 19, 1–12.

Feldman, G.C., Kuring, N., Ng, C., Esaias, W., McClain, C.R., Elrod, J., Maynard, N., Endres, D., Evans, R., Brown, J., Walsh, S., Carle, M., Podesta, G., 1989. Ocean color, availability of the global data set. Eos Transactions American Geophysical Union 70, 634–640.

Franz, B., 2006. Implementation of SST Processing Within the OBPG, ⟨http://oceancolor.gsfc.nasa.gov/DOCS/modis_sst/⟩ (accessed 18.10.11).

Fuentes-Yaco, C., Devred, E., Sathyendranath, S., Platt, T., Payzant, L., Caverhill, C., Porter, C., Maass, H., White, G.N., 2005. Comparison of in situ and remotely-sensed (SeaWiFS) chlorophyll-a in the Northwest Atlantic. Indian Journal of Marine Sciences 34 (4), 341–355.

Gagliardini, D.A., Rivas, A.L., 2004. Environmental characteristics of San Matías gulf obtained from Landsat-TM and ETM+ data. Gayana 68 (2), 186–193, TI.

Gaiero, D.M., Probst, J.L., Depetris, P.J., Leleyter, L., 2003. Iron and other transition metals in Patagonian riverborne and windborne materials: geochemical control and transport to the southern South Atlantic Ocean. Geochimica et Cosmochimica Acta 67, 3603–3623.

Garcia, C.A.E., Tavano Garcia, V.M.T., McClain, C.R., 2005. Evaluation of SeaWiFS chlorophyll algorithms in the Southwestern Atlantic and Southern Oceans. Remote Sensing of Environment 95, 125–137.

Garcia, V.M.T., Signorini, S., Garcia, C.A.E., McClain, C., 2006. Empirical and semi-analytical chlorophyll algorithms in the southwestern Atlantic coastal region (25–40°S and 60–45°W). International Journal of Remote Sensing 27, 1539–1562.

Gasso, S., Stein, A.F., 2007. Does dust from Patagonia reach the sub-Antarctic Atlantic Ocean? Geophysical Research Letters 34, L01801.

Glorioso, P.D., Simpson, J.H., 1994. Numerical modelling of the M2 tide on the Northern Patagonian shelf. Continental Shelf Research 14, 267–278.

González, R., Caille, G., Narvarte, M., 2007. An assessment of the sustainability of the hake Merluccius hubbsi fishery at San Matías gulf, Patagonia, Argentina. Fisheries Research (Elsevier) 87 (1), 58–67.

Gordon, H.R., Clark, D.K., 1980. Remote sensing optical properties of a stratified ocean: an improved interpretation. Applied Optics 19, 3428–3430.

Gordon, H.R., Morel, A.Y., 1983. Remote assessment of ocean color for interpretation of satellite visible imagery : a review. Springer-Verlag, New York 114.

Greenan, B.J.W., Petrie, B.D., Harrison, W.G., Oakey, N.S., 2004. Are the spring and fall blooms on the Scotian Shelf related to short-term physical events? Continental Shelf Research 24, 603–625.

Guerrero, R.A., Piola, A.R., 1997. Masas de agua en la plataforma continental. In: Boschi, E. (Ed.), El Mar Argentino y sus Recursos Pesquero, Tomo I: Antecedentes históricos de las exploraciones en el mar y las características ambientales. Instituto Nacional de Investigación y Desarrollo Pesquero. Mar del Plata, Argentina, pp. 107–119.

Hoffmann, J.A.J., Nuñez, M.N., Piccolo, M.C., 1997. Características climáticas del océano Atlántico Sudoccidental. El Mar Argentino y sus Recursos Pesqueros 1, 163–193.

Hooker, S.B., McClain, C.R., 2000. The calibration and validation of SeaWiFS data. Progress in Oceanography 45, 427–465.

Hovis, W.A., Clark, D.K., Anderson, F., Austin, R.W., Wilson, W.H., Baker, E.T., et al., 1980. NIMBUS-7 coastal zone color scanner—system description and initial imagery. Science 210, 60–63.

Longhurst, A., Sathyendranath, S., Platt, T., Caverhill, C., 1995. An estimate of global primary production in the ocean from satellite radiometer data. Journal of Plankton Research 17, 1245–1271.

Lutz, V.A., Subramaniam, A., Negri, R.M., Silva, R.I., Carreto, J.I., 2006. Annual variations in bio-optical properties at the 'Estación Permanente de Estudios Ambientales (EPEA)' coastal station, Argentina. Continental Shelf Research 26, 1093–1112.

Mann, K.H., Lazier, J.R.N., 1996. Dynamics of Marine Ecosystems. Biological–Physical Interactions in the Oceans, 2nd.ed.. Blackwell Science, Cambridge, USA.

McArdle, B.H., 1988. The structural relationship: regression in biology. Canadian Journal of Zoology 66, 2329–2339.

Montgomery, R.S., Strong, A.E., 1995. Coral bleaching threatens oceans, life. Eos Transactions of the AGU 75, 145–147.

Morel, A., Antoine, D., 2000. ATBD 2.9: Pigment Index Retrieval in Case 1 Waters. ESA, Noordwijk, The Netherlands, ESA Document no. PO-TN-MEL-GS-0005. Available from: ⟨http://envisat.esa.int/instruments/meris/pdf/atbd_2_09.pdf⟩ (accessed 17.01.07).

Morel, A., Prieur, L., 1977. Analysis of variations in ocean color. Limnology Oceanography 22, 709–722.

Morsán, E.M., 2003. Spatial analysis and abundance estimation of the southern-most population of purple clam, Amiantis purpurata in Patagonia (Argentina). Journal of the Marine Biological Association UK 83 (5), 1115–1128.

Narvarte, M., González, R., Filippo, P., 2007. Artisanal mollusc fisheries in the San Matías Gulf (Patagonia Argentina): an appraisal of the factors contributing to unsustainability. Fisheries Research (Elsevier) 87 (1), 68–76.

OReilly, J.E., Maritorena, S., Mitchell, B.G., Siegel, D.A., Carder, K.L., Garver, S.A., Kahry, M., McClain, C.R., 1998. Ocean color chlorophyll algorithms for SeaWiFS. Journal of Geophysical Research 103, 24937–24953.

Ocampo-Reinaldo, M., 2010. Evaluación pesquera integral de la merluza común (Merluccius hubbsi Marini, 1933) del Golfo San Matías y efectos de la explotación de esta especie sobre otros componentes de la trama trófica. Ph.D. Thesis. Universidad Nacional de Córdoba, Argentina, 156 pp.

O'Reilly, J.E., Maritorena, S., Siegel, D., O'Brien, M., Toole, D., Greg, B., Mitchell, Kahru M., Chavez, F., Strutton, P., Cota, G., Hooker, S., McClain, C., Carder, K., Muller-Karger, F., Harding, L., Magnuson, A., Phinney, D., Moore, G., Aiken, J., Arrigo, K., Letelier, R. and Culver, M., 2000. Ocean color chlorophyll-a algorithms for SeaWiFS, OC2, and OC4: version 4. In: O'Reilly, J.E., 24 coauthors, Hooker, S.B., Firestone, E.R. (Eds.), 2000: SeaWiFS Postlaunch Calibration and Validation Analyses, Part 3. NASA Technical Memorandom 2000-206892, vol. 11. NASA Goddard Space Flight Center, Greenbelt, Maryland, pp. 9–23.

Otero, L., Ristori, P., D'Elia, R., Rosales, A., Quel, E., 2009. Dust over the Patagonia Argentina, March 2009. ANALES AFA 21, 272–275, Rosario.

Otero, L., Ristori, P., Que, B., 2006. Aerosol optical thickness at ten AERONET—NASA stations during 2002. Óptica Pura y Aplicada. 39 (4), 355–364.

Palma, E.D., Matano, R.P., Piola, A.R., 2004. A numerical study of the South Western Atlantic Shelf circulation: barotropic response to tidal and wind forcing. Journal of Geophysical Research 109, C08014, http://dx.doi.org/10.1029/2004JC002315.

Piola, A.R., Scasso, L.M.L., 1988. Circulación en el Golfo San Matías. Geoacta 15 (1), 33–51.

Rivas, A., Beier, E., 1990. Temperature and salinity fields in the Northpatagonic Gulfs. Oceanologica Acta 13, 15–20.

Rivas, A.L., 2010. Spatial and temporal variability of satellite-derived sea surface temperature in the southwestern Atlantic Ocean. Continental Shelf Research 30, 752–760.

Rivas, A.L., Dell'Arciprete, P., 2000. Frentes térmicos en la plataforma Patagónica inferidos a partir de datos satelitales. IV Jornadas Nacionales de Ciencias del Mar, Resúmenes, 107 pp.

Romero, M.A., González, R., Ocampo Reinaldo, M., 2010. When conventional fisheries management measures fails to reduce the catch and discard of juvenile fish: a case study of Argentine hake trawl fishery in San Matías Gulf. North American Journal of Fisheries Management 30, 702–712.

Santos, A.M.P., 2000. Fisheries oceanography using satellite and airborne remote sensing methods: a review. Fisheries Research 49, 1–20.

Saraceno, M., Provost, C., Piola, A.R., 2005. On the relationship between satellite-retrieved surface temperature fronts and chlorophyll-a in the western South Atlantic. Journal of Geophysical Research 110, C11016, http://dx.doi.org/10.1029/2004JC002736.

Sastre, A.V., Santinelli, N.H., Esteves, J.L., 1997. Fitoplancton del Golfo San Matías de tres campañas de muestreo (Noviembre de 1992, Septiembre de 1993, Marzo de 1994). Physis (Buenos Aires Section A53 (124–125), 7–12.

Sathyendranath, S., Cota, G., Stuart, V., Maass, H., Platt, T., 2001. Remote sensing of phytoplankton pigments: a comparison of empirical and theoretical approaches. International Journal of Remote Sensing 22, 249–273.

Sathyendranath, S., Lazzara, L., Prieur, L., 1987. Variations in the spectral values of specific absorption of phytoplankton. Limnology and Oceanography 32, 403–415.

Scasso, L., Piola, A., 1988. Intercambio neto de agua entre el mar y la atmósfera en el Golfo San Matías. Oceanologica Acta 15 (1), 13–31.

Sokal, R., Rholf, F.J., 1995. Biometry. W.H. Freeman and Company, New York 408 pp.

Strickland, J.D.H., Parsons, T.R., 1972. A Practical Handbook of Seawater Analysis, Second Edition. Bulletin 167. Fisheries Research Board of Canada, Ottawa 311 pp.

Stuart, V., Sathyendranath, S., Platt, T., Heide, Maass, Irwin, B.D., 1998. Pigments and species composition of natural phytoplankton population: effect on the absorption spectra. Journal of Plankton Research 20 (21), 187–217.

Stumpf, R.P., Arnone, R.A., Gould Jr., R.W., Martinolich, P.M., Ransibrahmanakul, V., 2003. A partially coupled ocean–atmosphere model for retrieval of water-leaving radiance from seawifs in coastal waters. NASA Technical Memoran-dom 206892, National Aeronautics and Space Administration. Goddard Space Flight Center, Greenbelt, MD.

Szeto, M., Werdell, P.J., Moore, T.S., Campbell, J.W., 2011. Are the world's oceans optically different? Journal of Geophysical Research 116, C00H04, http://dx.doi.org/10.1029/2011JC007230.

Tonini, M., Palma, E., Rivas, A., 2006. In: Alberto, Cardona, Norberto, Nigro, Victorio, Sonzogni, Mario, Storti (Eds.), Modelo de alta resolución de los golfos patagónicos, vol. XXV. Mecánica Computacional, pp. 1441–1460 42.

Tonini, M., Palma, E.D., Rivas, A.L., 2007. Simulación numérica de la circulación y Frentes Térmicos en los golfos Norpatagónicos. Mecánica Computacional 26, 3757–3768.

Werdell, P.J., Bailey, S.W., Franz, B.A., Harding Jr., L.W., Feldman, G.C., McClain, C.R., 2009. Regional and seasonal variability of chlorophyll-a in Chesapeake Bay as observed by SeaWiFS and MODIS-Aqua. Remote Sensing of Environment 113, 1319–1330.

Williams, G.N., 2004. ¿Cuáles son las Fuentes de nutrientes para mantener la productividad del golfo San Matías? Tesis de grado. Universidad Nacional de la Patagonia San Juan Bosco, Puerto Madryn, Argentina, 100 pp.

Williams, G.N., Sapoznik, M., Ocampo-Reinaldo, M., Solís, M., Narvarte, M., González, R., Esteves, J.L., Gagliardini, D.A., 2010. Comparison of AVHRR and SeaWiFS imagery with fishing activity and in-situ data in San Matías Gulf, Argentina. International Journal of Remote Sensing 31 (17), 4531–4542.